BACKSCATTER SIGNAL MODEL
FOR IRKUTSK INCOHERENT SCATTER RADAR

V.P. Tashlykov
Institute of Solar-Terrestrial Physics SB RAS,
Irkutsk, Russia, vtashlykov@iszf.irk.ru

A.V. Medvedev
Institute of Solar-Terrestrial Physics SB RAS,
Irkutsk, Russia, medvedev@iszf.irk.ru

R.V. Vasilyev
Institute of Solar-Terrestrial Physics SB RAS,
Irkutsk, Russia, roman_vasilyev@iszf.irk.ru

Abstract. The paper presents a backscatter signal model for Irkutsk Incoherent Scatter Radar (IISR) and proposes a technique for solving the inverse problem of determining plasma temperatures from IISR data. This solution is validated by setting up the direct scattering problem and simulating it using the Monte-Carlo method. In addition, we can introduce known systematic error sources into the backscatter signal model. This enables us to determine which approaches can be used to recover temperatures correctly. The major task of this study is to identify and methodically correct the errors that can distort the obtained temperatures. We also report the results of testing of the developed technique for determining temperatures from IISR experimental data. The presented model and IISR experimental data can be used to validate techniques for determining other ionospheric plasma parameters.

Keywords: ion and electron temperatures, incoherent scatter technique, incorrect inverse problems.

INTRODUCTION

Irkutsk incoherent scatter radar (IISR) is one of the most informative instruments of ground-based remote sensing of ionosphere over Siberian region. The IISR history dates back to 1993 when the radar array "Dnepr" was converted for scientific use. Owing to comprehensive modernization of receiving, acquisition, processing, and control equipment, the diagnostic capability of the radar has significantly increased [Potekhin et al., 2009]. From the initial radar array, IISR got an antenna system that represents an H-sectorial horn fed by a slotted-guide system with a ribbed slow-wave structure [Zherebtsov et al., 2002]. This system can radiate a signal with single linear polarization in a range 154-162 MHz, which is not traditional for the incoherent scatter (IS) method and creates additional difficulties in determining ionospheric plasma parameters.

The incoherent scatter method involves receiving and processing a signal that scatters back to the radar from the ionosphere after a given sequence of short pulses is radiated. Unlike the traditional radiolocation in which the subject of interest is a range to a point object, IS radars explore the ionosphere, which is a space-distributed object covering the whole radar scope. Thus, the space-time configuration of scattering should be accounted for in signal processing (Figure 1). Statistical characteristics of the backscatter signal illustrate physical conditions of ionospheric plasma: altitude profiles of electron density, electron and ion temperatures, ion drift, etc.

The backscatter signal forms as a result of interference of signals scattered by thermal fluctuations of plasma permittivity. Such fluctuations are generally assumed to be stochastic with Maxwellian distribution of electron thermal velocities. The IS theory was developed from this approach [Evans, 1969]; and the known
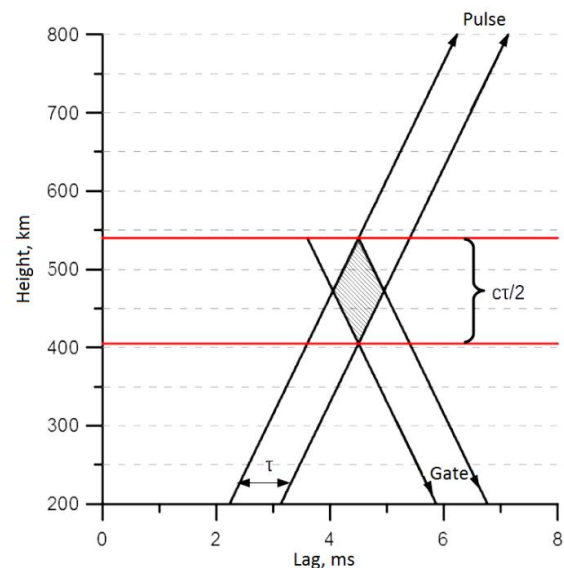
Figure 1. Space-time configuration for scattering pulse with τ duration

electron velocity distribution enables us to derive analytically the expression for spectrum of a signal scattered in plasma [Sheffield, 1978]. Actually, electron motions in ionospheric plasma are not fully independent, that is, their trajectories partially correlate. Furthermore, the correlation scale depends on the ratio of Debay length to radar wavelength, electron and ion temperatures, as well as on the exterior magnetic field. There are so-called "collective effects" — manifestations of space and time correlation between plasma particles, which can distort the backscatter signal spectrum shape by coherent scatter component leading to an increase in the systematic error. Nevertheless, complica-

tions arising from the collective effects and distorting backscatter signal spectra can provide a large amount of additional information about the ionosphere with a correct direct problem model [Kudeki, Milla, 2012].

Due to the random nature of thermal plasma fluctuations, spectra or autocorrelation functions (ACF) of a received signal should be averaged over a period during which the ionosphere is considered unaltered. In practice, obtaining the spectrum with sufficient variance requires averaging (depending on a signal-to-noise ratio) over 2000 realizations, i.e. transmitting-receiving cycles. For IISR, the sounding pulse duration is from 200 to 900 μs, and the period of signal registration is ~8 ms that corresponds to a range of 1200 km. With a pulse repetition rate of 24.4 Hz and a duty cycle of ~20 %, it takes about 5 min to accumulate 3-4 thousands of realizations. Figure 1 shows that the space resolution of the experiment depends on the sounding pulse duration.

The major task of this study is to develop an algorithm for finding and removing systematic errors of the IS method. The algorithm must account for design features of IISR, viz. the presence of a single linear polarization. The proposed algorithm is based on the backscatter signal model, which has been adopted to study the IISR capability of using code pulse sequences to reconstruct the electron density profile [Alsatkin et.al., 2009]. We place emphasis on the single pulse regime, which is used to reconstruct temperature profiles. The proposed method can be further developed to estimate other ionospheric plasma parameters such as ion composition, direction and amplitude of drift velocity and plasma electric fields. It also has great potential for studying ionospheric irregularities because they cause collective effects whose interpretation in the backscatter signal model is sufficiently simple.

STATEMENT OF THE PROBLEM

A proper determination of electron and ion temperatures of ionospheric plasma is one of the most relevant tasks of the IISR research team. Development of a temperature recovery technique for IISR encounters difficulties related to the radar antenna design. The single linear polarization impedes the recovery of the continuous temperature profile because of distinctive signal fadings caused by the Faraday effect. When a linearly polarized signal propagates through a medium along a magnetic field, the polarization plane rotates throughout the signal propagation path, and the rotation velocity, to a first approximation, depends on electron density. On the one hand, this effect enables us to determine the electron density profile without calibration from ionosonde data, as opposed to IS radars with circle polarization. On the other hand, when the polarization plane is perpendicular to the polarization filter, there are signal fadings with much lower signal-to-noise ratio.

In the ionospheric observation regime, IISR successively radiates two pulses with different frequencies: the first one is amplitude-modulated with a duration of 700 μs, the second one is phase-manipulated (Barker code) with a duration of 200 μs. In 2013, IISR started using the regime of successive radiation and reception of two

700 μs and 900 μs pulses. Applying the effective subtraction technique [Berngardt et al., 2013] to the data, we can achieve higher spatial resolution of the measured parameters. A backscatter signal from each pulse is received by independent channels: narrowband (700 and 900 μs) and wideband (200 μs). The narrowband signal has high spectral resolution. This enables us to recover plasma parameters associated with ion-acoustic spectral line. The receiving gate duration is usually equal to the sounding pulse duration, which defines the spectral resolution. The gate processing allows us to assess ACF that is sufficient to determine electron and ion temperatures. The accuracy of the ACF assessment depends on the signal-to-noise ratio and the systematic errors, which can be taken into account only using a reliable physical model of signal scattering and reception.

The wideband signal provides information about signal power with high spatial resolution of 6 km. This allows us to reconstruct the electron density profile using the Faraday fading phase. The electron density determining technique for IISR is described in [Ratovsky et al., 2017]. During the electron density reconstruction, we derive the model profile of signal fadings (Figure 2).

Another important IISR feature is its ~2 m wavelength. As is known from the IS theory, ionospheric irregularities of the typical scale comparable to the radar wavelength can generate the coherent component of the backscatter signal. IS radars generally have a wavelength much shorter than 1 m, which is much smaller than the minimum irregularity scale associated, for example, with spread-F. The technique for identifying mid-latitude irregularities for IISR wavelengths and the assessment of their related systematic errors are subjects of future research. The main task of this study is to develop a temperature determination algorithm eliminating systematic errors caused by the Faraday effect.

To solve this problem, we should address three subtasks. The first subtask is to derive a radar equation that relates spectral or correlation characteristics of the received signal to corresponding characteristics of plasma. The radar equation for different approximations has been derived in [Berngardt and Potekhin, 2000; Shpynev, 2004]. The second subtask is to find a stable solution of the radar equation, which, like most geophysical problems, is an ill-posed inverse problem. Holt et al. [1992] proposed an OASIS technique (Optimal Analysis of Signals from Incoherent Scatter) — fitting the full height profiles of parameters under study (density,
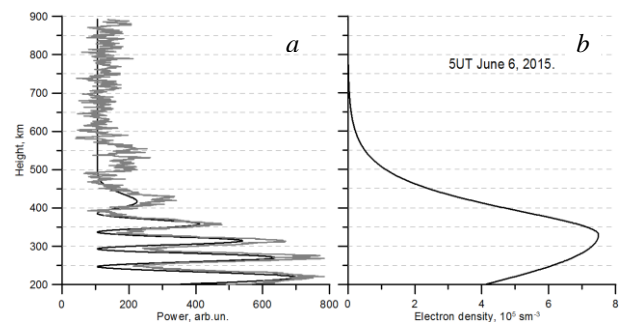
Figure 2. Comparison between experimental wideband signal power and model power profile (*a*); recovered electron density profile (*b*)

temperatures, ion composition) to experimental ACF values, using the least squares method. This technique was successfully applied to the IS radars Millstone Hill and Jicamarca Radio Observatory [Hysell et al., 2008]. Another approach relies on the statistical theory of inverse problems [Tarantola, 1987; Lehtinen, 1986] and considers IS data as random Gaussian variables; the authors use the Bayesian approach to solve the radar equation. The solution of the third subtask is closely connected with the solution of the second subtask and defines how close the physical spectral model is to experimental data.

DERIVING RADAR EQUATION

We propose a backscatter signal model that interprets the medium as uniformly distributed set of "scatterers" that reflect a signal with a random phase (according to the uniform distribution) and with an amplitude proportional to the amplitude of plasma fluctuation power spectrum at a given frequency. In this representation, the backscatter signal consists of signals reflected from the "scatterers". As a scattering spectrum model we use expressions from [Sheffield, 1978] for cold collisionless plasma with O+ ion species.

The received signal power depends above all on electron density and polarization plane orientation relative to the radar polarization filter. The direct problem model represents it as amplitude modulation of backscatter signal, using an experimental wideband power profile.

To solve the stated problem, we propose a mathematical model for backscatter signal formation. The expression can be written as

$$s(t) = \sum_h F(h) Q\left(h - \frac{ct}{2}\right) \sum_{n=0}^{N} S_{nh} = e^{i(\omega_{nh} t + 2k_{nh} h + \varphi_{nh})}, \quad (1)$$

where $F(h)$ is the Faraday fading profile; S_{nh}, ω_{nh}, k_{nh} are the amplitude, frequency, and wave number of the plasma scattering spectrum for the n-th scatterer and height h respectively; φ_{nh} is the random scattering phase, Q is the sounding pulse envelope. This expression is derived in the approximation of the radar pulse response to the delta-function (for active IISR experiments, a frequency band is 125 kHz), which reduce the Duhamel integral for expression (1). The function $f(t)$ represents the model of a quadarature signal received by a heterodyne receiver. The sounding pulse shape is considered to be an ideal rectangle.

The radar equation for signal ACF can be constructed based on technical features of IISR and specificity of the problem under study. The comparison between the derived equation and the traditional IS equation [Farley, 1969] allows us to infer that our scattering interpretation is correct. For a stationary random process, the ACF signal with the gate function $o(t)$ is

$$R(\tau) = \sum_t s(t) o(t) s^*(t - \tau) o(t - \tau). \quad (2)$$

The expression represents the signal ACF of a single realization and does not yet relate it to the plasma fluctuation ACF. However, using the following properties of the sum and phase distribution, we can simplify this expression (see Appendix), thus obtaining the inverse Fourier transform of scattering power spectrum in plasma. According to the Weiner — Khinchin theorem, this component represents the plasma scattering ACF.

After averaging this expression, its three last components vanish provided that the phase φ is uniformly distributed. So, the averaged signal ACF reduces to

$$R(\tau, h) = \sum_{t=\tau}^{T} \left\{ \sum_h \left[F^2(h) w(\tau, t, h, h) \sum_{n=0}^{N} S_{nh}^2 e^{2i\omega_{nh}\tau} \right) \right] \right\} =$$

$$= \sum_{t=\tau}^{T} \left\{ \sum_h \left[F^2(h) w(\tau, t, h, h) R_0(\tau, h) \right] \right\}, \quad (3)$$

where R_0 is the inverse Fourier transform (ACF) of the plasma fluctuation power spectrum. The resulting radar equation agrees with that derived in [Farley, 1969] and, besides, accounts for the Faraday effect in the direct problem model for signal with single linear polarization. The approximations used for the radar equation are of practical importance because the neglected impulse response introduces much lower error than the Faraday effect.

RADAR EQUATION SOLUTION

The derived radar equation can be resolved to the system of τ-independent linear equations. The main difficulty is that the problem is ill-posed. This requires regularizing the solution and involving the maximum amount of data from other instruments and a priori constraints. Such an approach was used in [Lehtinen, 1986; Holt et al., 1992]. Its major disadvantage is that systematic errors are ignored when the physical model does not describe actual ionospheric phenomena. Signal variance increases with height rather rapidly since the power of a signal received with a monostatic radar is proportional to r^2 (range), and the integration time is restricted to the period of stationarity of the ionosphere. As a result, the full-profile analysis uses ranges that provide no physical information. The problem is therefore equally important for both the stable solution of the inverse problem and the search for systematic errors ignored in the direct problem. That is why we propose a controllable reduction of the radar equation, which allows us to quickly estimate the solution at a first approximation:

$$R_0(\tau) = \frac{R(\tau)}{W(\tau)}, \quad (4)$$

where

$$W(\tau) =$$

$$\sum_{t=\tau}^{T} \left\{ \sum_h \left[F^2(h) Q\left(h_1 - \frac{ct}{2}\right) Q\left(h_2 - \frac{ct}{2} + \frac{c\tau}{2}\right) o(t) o(t - \tau) \right] \right\}$$

is the weight function, also called the ambiguity function in the IS theory. The function $W(\tau)$ decreases monotonically in the positive domain of τ, has a maximum value at τ=0, and vanishes at τ equal to the sounding pulse duration. The proposed approach is perspective with a view of searching for additive scattering sources as applied to IISR experimental data.

RELATION OF TEMPERATURES TO SCATTERING SPECTRUM

The plasma permittivity fluctuation spectrum is analytically formulated by Sheffield [1978]:

$$S(k_s,\omega) = \frac{2\pi}{k_s}\left|1-\frac{G_e}{\epsilon}\right|^2 f_{e_0}\left(\frac{\omega}{k_s}\right) + \frac{2\pi Z}{k_s}\left|\frac{G_i}{\epsilon}\right|^2 f_{i_0}\left(\frac{\omega}{k_s}\right), (5)$$

where k_s is the wave number, f_0 is the radar operating frequency, Z is the ion charge,

$$f_{e_0}(\nu) = \frac{\exp\left(-\frac{\nu^2}{a^2}\right)}{\left(\pi a^2\right)^{\frac{1}{2}}} \quad \text{and} \quad f_{i_0}(\nu) = \frac{\exp\left(-\frac{\nu^2}{b^2}\right)}{\left(\pi b^2\right)^{\frac{1}{2}}}$$

are the electron and ion velocity distributions for thermodynamic equilibrium (Maxwell distribution) respectively; $a=(2k_bT_e/m_e)^{1/2}$ and $b=(2k_bT_i/m_i)^{1/2}$ are the thermal velocities of electrons and ions respectively (k_b is the Boltzmann constant);

$$G_e = \alpha^2\left(1-2x_e e^{-x_e^2}\int_0^{x_e} pe^{p^2}dp - i\pi^{1/2}x_e e^{-x_e^2}\right) \text{ and}$$

$$G_i = \alpha^2\left(1-2x_i e^{-i_e^2}\int_0^{x_e} pe^{p^2}dp - i\pi^{1/2}x_i e^{-x_i^2}\right)$$

are the Gordeev integrals for nonmagnetized plasma; $\alpha=1/k\lambda_D$, $x_e=\omega/ka$, $x_i=\omega/kb$, $\epsilon=1+G_e+G_i$, and λ_D is the Debay length.

This subtask can be solved by fitting plasma fluctuation spectra to analytical ones, which are reliably related to plasma parameters. This approach is, however, not fully justified as regards the number of calculations needed. It's enough to estimate some ACF characteristic values (lags of the first zero in positive lag domain as well as lag and amplitude of the first minimum [Rogozhkin, 1979]) and to relate these parameters to plasma temperatures.

The regression was carried out on the basis of least squares technique using the Gauss-Newton method. The approximation of the desired function is adjusted at each iteration as

$$f(\beta,x) = f(\beta_0,x) + \mathbf{J}_0(\beta-\beta_0), \quad (6)$$

where $\mathbf{J}_0$ is the Jacobian of function f.

The iterative estimation of vector $\boldsymbol{\beta}$ is obtained from

$$\boldsymbol{\beta}_{j+1} = \boldsymbol{\beta}_j + \left(\mathbf{J}_0^T\mathbf{J}_0\right)^{-1}\mathbf{J}_0^T\mathbf{e}, \quad (7)$$

where $\mathbf{e}$ is the residual vector for the j-th iteration.

The regression yields expressions for determining T_e and $T_r=T_e/T_i$

$$T_e \approx 1.9\cdot10^8\frac{1}{\tau_0^2} + 1.12\cdot10^5\frac{1}{\tau_0} - 2.2\cdot10^8\frac{1}{\tau_{min}^2} +$$

$$+2.03\cdot10^5\frac{1}{\tau_{min}} - 24,$$

$$T_r \approx 13.8A_{min}^2 - 0.04A_{min} + 0.5, \quad (8)$$

where τ_0, τ_{min}, A_{min} are the real ACF first zero lag, lag and amplitude of the first minimum, respectively. Since IISR radiates and receives signals in the frequency range 154–162 MHz, it is necessary to insert running parameters accounting for the radar wavelength into the regression. Expression (3) includes the radar wavelength as $1/\lambda$ factor (k_s) and as the parameters of nonlinear functions f_{e0} and f_{i0} as well, but, as seen in Figure 3, this nonlinear dependence can be neglected. The ACF parameters should, therefore, be normalized to a wavelength of 2 m.

$$t_0 = t_0'\frac{\lambda_0}{\lambda},$$

$$t_{min} = t_{min}'\frac{\lambda_0}{\lambda}, \quad (9)$$

where $\lambda_0=2m$, λ is the current radar wavelength, t_0' and t_{min}' are lags of the real ACF first zero and minimum.

Figure 4 shows the estimated regression error. The maximal deviation is less than 10 %, which is acceptable for the experimental signal-to-noise ratio $\ll 1$. The regression error exceeds 5 % for ion and electron temperatures, which actually are extrinsic for ionospheric plasma in the height range observed by IISR.

The derived solution for the inverse problem can be examined by simulating the backscatter signal formation.

SIMULATION

The statement of the direct problem defines the backscatter signal formation to be simulated. To obtain the average ACF from (2), we should sum up several thousands of quadrature ACF for independent realizations. This problem requires enormous computational power; therefore we make calculations using data from the high-performance computing center "Academic V.M. Matrosov" [http://hpc.icc.ru]. Parallelization of the calculations allows us to reach multiple acceleration of simulation.

After ACF averaging, we use equations (2) and (4) and compare the model input and recovered temperatures. The model input represents linear gradients of electron and ion temperatures, as well as signal power fadings obtained experimentally using a wideband IISR signal. When the signal power fadings are ignored in the solution of the radar equation, the recovered temperature profiles are inconsistent with the expected ones.
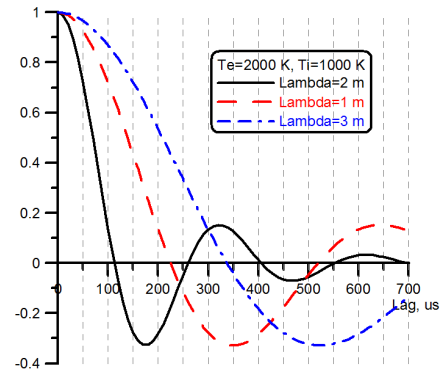
Figure 3. Plasma fluctuation ACF for 1, 2, and 3 m wavelengths
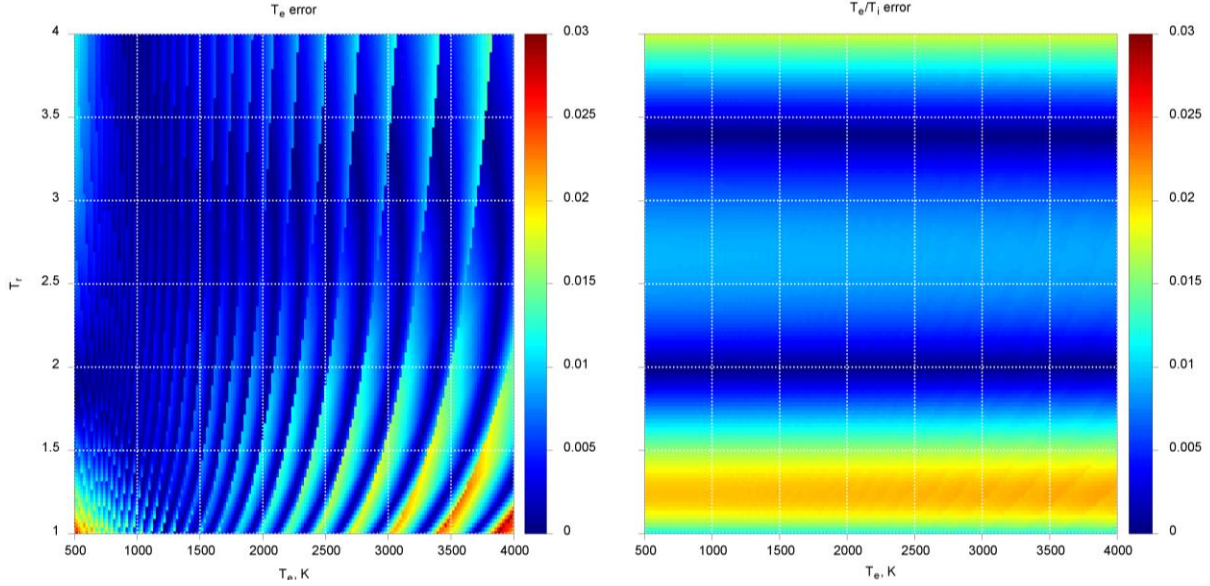
Figure 4. Deviation of the regression from scattering spectrum model (Equation (8))
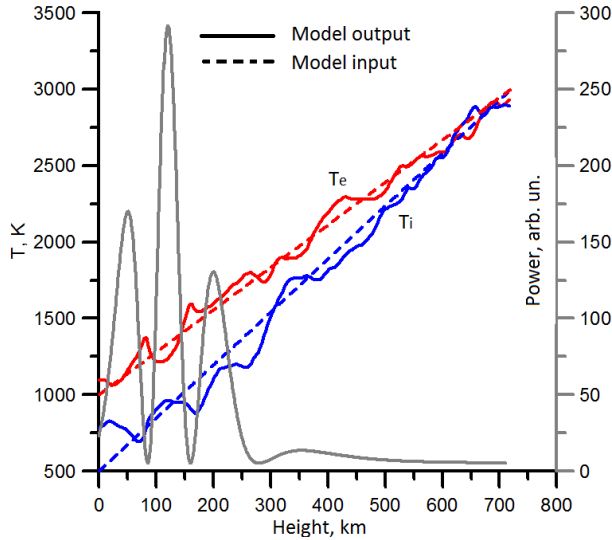
Figure 5. Comparison between input and recovered temperatures for characteristic IISR Faraday profile

Figure 5 shows the comparison between the model input and the temperature profiles recovered with due account for signal fadings. The maximum error of ~10 % for T_e and ~20 % for T_i are acceptable for the statistics of ~2000 realizations.

To examine if the algorithm eliminates the systematic error from signal fadings, we have accumulated ~100000 realizations, with the kernel of random sequences changed for every 300 realizations. Then, ACF of the simulated signal realizations were averaged over 2000 realizations. For the same model input (Figure 6), the recovered temperatures repeated the expected behavior with relatively constant variance.

Figure 6 presents profiles of characteristic ACF values for sounding pulse duration of 700 μs: *a*, *b*, and *c* are the actual ACF lag of the first zero, lag and amplitude of the first minimum respectively, before being inversed by equation (2); *d*, *e*, and *f* are the actual ACF lag of the first zero, lag and amplitude of the first mini-

mum respectively, after being inversed by equation (2). As seen in Figures 6*b* and 6*c*, the input Faraday fading profile distorts the ACF form, introducing peculiar dips in the parameters. At the same time, the ambiguity function amplitude has similar peculiarities, and after using equation (4), we recover the temperature profiles that agree with the input ones (Figures 6*e* and 6*f*). The minor difference of the first zero behavior (Figures 6*a* and 6*b*) indicates the validity of the assumed approximation, which implies the multiplicative character of the inverse problem solution.

VALIDATION OF THE DEVELOPED TEMPERATURE RECOVERY TECHNIQUE FROM IISR EXPERIMENTAL DATA

The proposed algorithm for temperature recovery has no regularization; therefore, the experimental solution is unstable and does not allow us to obtain the correct temperatures from IISR data in a number of circumstances. First, in presence of small-scale ionospheric irregularities, a backscatter signal can comprise strong interference distorting the signal ACF. Second, the signal-to-noise ratio decreases at low electron density, which leads to a small number of signal fadings. In this case, the required integration time can exceed the ionosphere stationarity time.

Nevertheless, the developed technique has been examined from the IISR experimental data for summer days at low geomagnetic activity when the number of signal fadings is large enough and their width is less than the pulse duration. This causes a relatively weak distortion of the obtained temperature profiles by the Faraday effect. Figure 7 shows the recovered temperatures and electron density for June 11–15, 2015. The diurnal behavior of the obtained temperatures agrees with the expected one.

Figure 8 presents the comparison between the time variation of the ion temperatures derived from IISR data

28
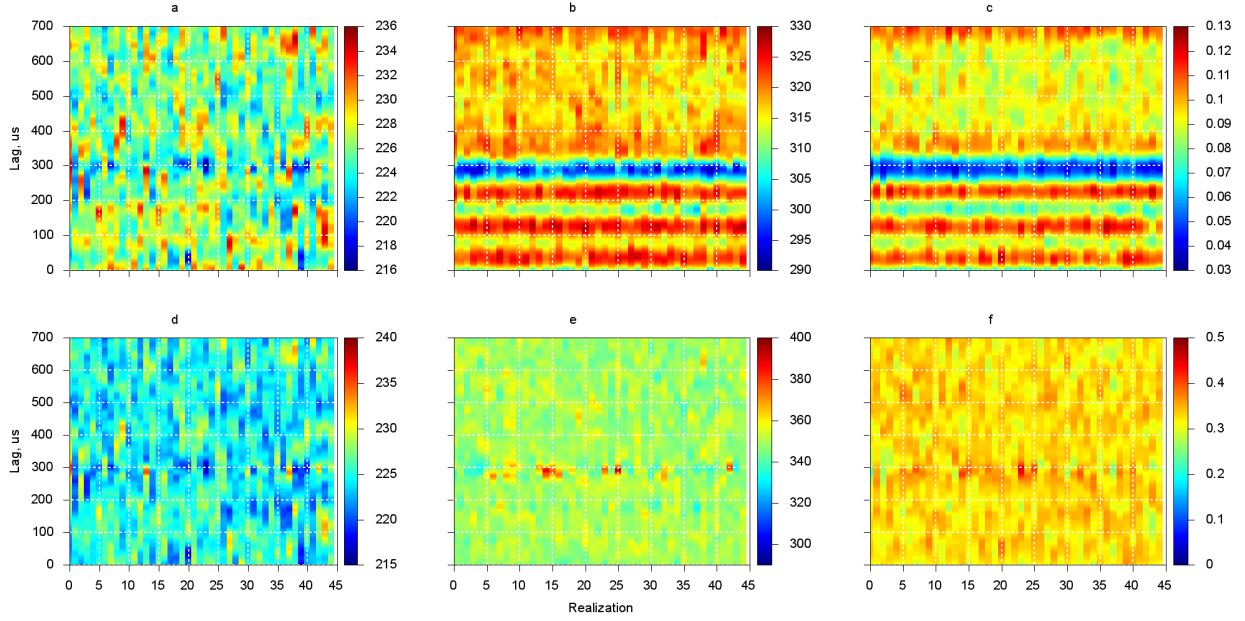
Figure 6. $\tau_0 (<R(\tau)>)$ (*a*); $\tau_{min} (<R(\tau)>)$ (*b*); $A_{min} (<R(\tau)>)$ (*c*); $\tau_0 (R_0(\tau))$ (*d*); $\tau_{min} (R_0(\tau))$ (*e*); $A_{min} (R_0(\tau))$ (*f*)
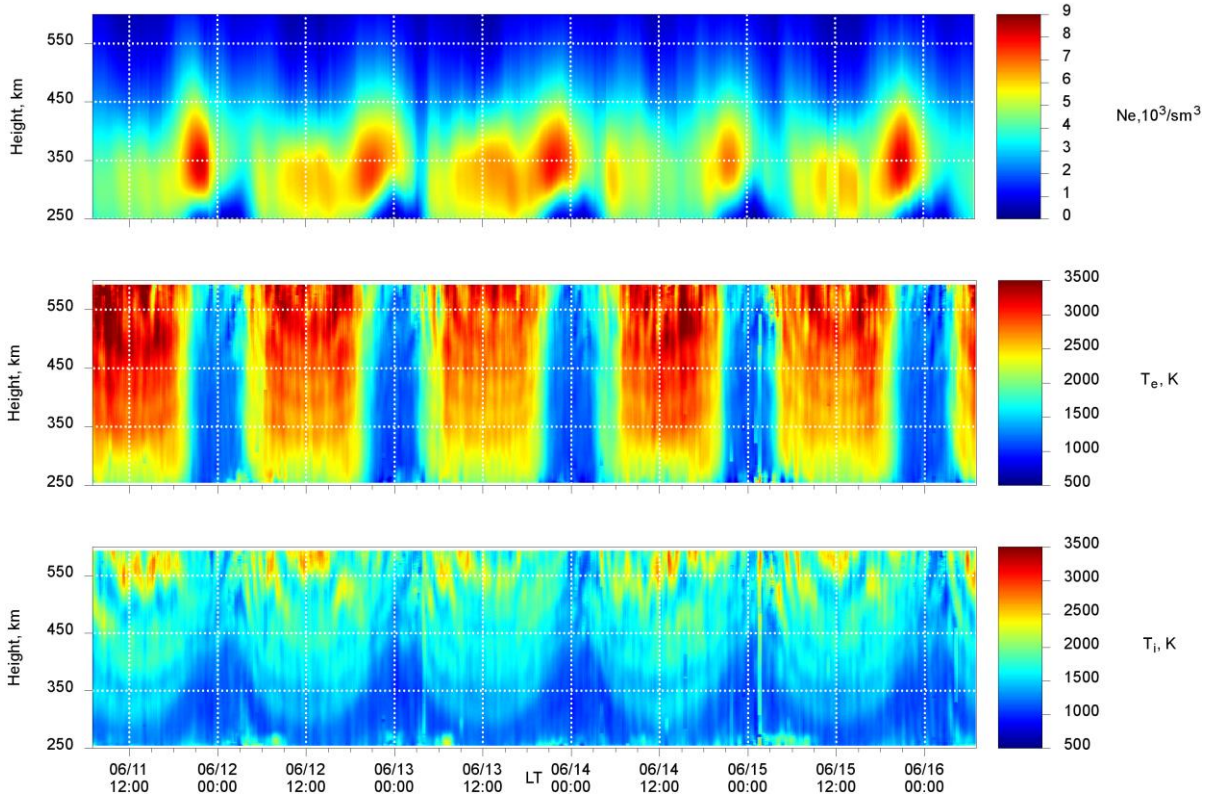
Figure 7. Electron density, electron and ion temperatures as derived from the IISR data for June 11-15, 2015

and the neutral temperature obtained from the data acquired with the Fabry — Perot interferometer located in Tory [Vasilyev et.al., 2017].

Thus, after excluding possible technical errors of data processing, we should set up the problem of searching for other systematic errors. From the data analysis, we propose hypotheses explaining the presence of systematic errors ignored before.

1. The weight function for (2) is obtained incorrectly because of input data ambiguity, i.e. the wideband signal power profile. At ranges over 400 km, the low

signal energy (the pulse duration is 200 µs that corresponds to the 30 km height range) does not allow us to identify Faraday variations, which certainly contributes to the signal ACF. Moreover, the value of power dips, strictly speaking, can be nonzero and height dependent.

2. The approximation for equation (2) causes an error at strong temperature gradients. However, the algorithm validity was examined on the basis of simulation for different temperature gradients. In each case, correct temperatures were obtained.
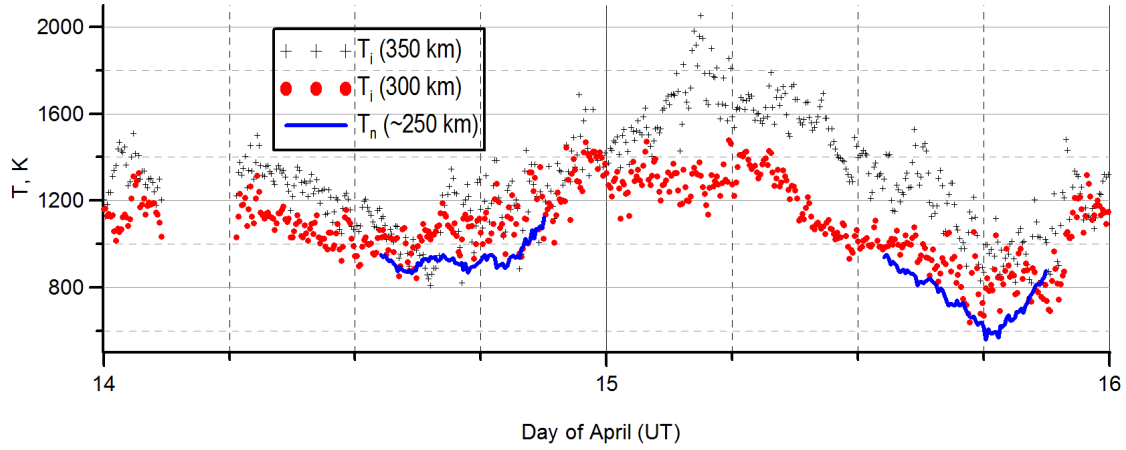
Figure 8. Comparison between ion temperatures derived from IISR and neutral temperatures obtained with the Fabry-Perot interferometer

3. Other important property is the character of the ambiguity function for a monostatic radar in the presence of the Faraday effect (see Figures 9 and 10). For the gate signal processing, the center of the exposed ionospheric volume is located at the gate start because both current and prior gates contribute to the resulting ACF. By comparison, we have chosen heights of 300 and 350 km for 4 and 15 UT of April 15, 2016.

Figure 9 shows that the major ACF contribution is made by heights, which are much lower than that of the gate start. When averaging ACF with significantly different energies, ACF of the highest energy makes a major contribution. As a result, the obtained temperatures correspond to the ambiguity function "mass center", which can locate either higher or lower than the gate start (see Figure 9). There may be a complete ambiguity (as in Figure 10 for 300 km height) when there are two "mass centers" with its own temperatures each. The resulting temperature for the gate of 300–405 km corresponds to the weighted average of temperatures at ~210 and ~320 km.

Such an interpretation gives no insight into actual temperatures at 300 km exactly. Perhaps, the Faraday effect prevents gaining any information about temperatures at heights of signal fadings locate.

Figure 9. Ambiguity function amplitude for gates at heights of 300 and 350 km on April 15, 2016, at 4 UT
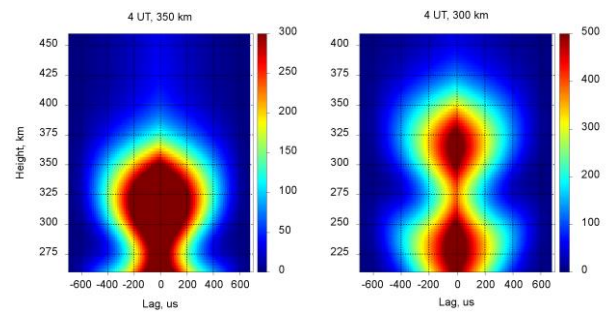
Figure 10. Ambiguity function amplitude for gates at heights of 300 and 350 km on April 15, 2016, at 15 UT

CONCLUSION

The proposed technique for solving the inverse problem from backscatter signal simulation provides a fast and comprehensive approach to develop techniques for determining plasma parameters such as electron and ion temperatures, plasma drift velocity, electric fields, ion composition, etc. At quiet geomagnetic activity and high electron density, the technique reliably yields diurnal variations of electron and ion temperatures. In other cases, the inverse problem approach in use is insufficient to enable us to obtain reliable temperatures. A more rigorous approach to the inverse problem solution suggests decomposing the radar equation to a system of linear equations and applying regularization techniques (for instance, Tikhonov regularization). This algorithm is under development.

To solve the inverse problem, we can drop from any approximation for the radar equation solution provided that the analysis involves a priori constraints and measurement data from other instruments. We can also leave out direct problem approximations and derive the radar equation in the most expanded form. This proves worthwhile with acceptable computation capabilities only for the first-approximation solution and clear comprehension of physical phenomena introducing systematic errors into the experiment. The proposed backscatter signal model provides such a solution. Hypothesizing sources of systematic errors, we can perform fast and effective estimation of its validity on the basis of simulation.

APPENDIX

Denoting expression $S_{nh}e^{i(\omega_{nh}t+2k_{nh}h+\varphi_{nh})}$ as $x(t,n,h)$ and expression $Q\left(h_1-\dfrac{ct}{2}\right)Q\left(h_2-\dfrac{ct}{2}+\dfrac{c\tau}{2}\right)o(t)o(t-\tau)$ as $w(\tau,t,h_1,h_2)$, we obtain

$$R(\tau)=\sum_{t=\tau}^{T}\left\{\left[\sum_h F(h)x(t,n,h)Q\left(h-\frac{ct}{2}\right)o(t)\right]\left[\sum_h F(h)\sum_{n=0}^{N}x^*(t-\tau,n,h)e^{i\omega_{nh}\tau}Q\left(h-\frac{c(t-\tau)}{2}\right)o(t-\tau)\right]\right\}.$$

Using the sum property $\sum_x A_x \sum_x B_y=\sum_x\sum_y A_x B_y$, modify:

$$R(\tau)=\sum_{t=\tau}^{T}\left\{\sum_{h_1}\sum_{h_2}\left[F(h_1)F(h_2)w(\tau,t,h_1,h_2)\sum_{n=0}^{N}x(t,n,h)\sum_{n=0}^{N}x^*(t-\tau,n,h)e^{i\omega_{nh}\tau}\right]\right\}=$$

$$=\sum_{t=\tau}^{T}\left\{\sum_{h_1}\sum_{h_2}F(h_1)F(h_2)w(\tau,t,h_1,h_2)\sum_{n_1=0}^{N}\sum_{n_2=0}^{N}\left[x(t,n_1,h_1)x^*(t-\tau,n_2,h_2)e^{i\omega_{n_2h_2}\tau}\right]\right\}=$$

(Then, apply the sum property $\sum_x\sum_y A_x B_y=\sum_x A_x B_x+\sum_x\sum_{y\neq x}A_x B_y$ successively to n and h):

$$=\sum_{t=\tau}^{T}\left\{\sum_{h,\,h_2=h_1}\left[F^2(h)w(\tau,t,h,h)\sum_{n_1=0}^{N}\sum_{n_2=0}^{N}\left[x(t,n_1,h_1)x^*(t-\tau,n_2,h_2)e^{i\omega_{n_2h_2}\tau}\right]\right]\right\}+$$

$$+\sum_{t=\tau}^{T}\left\{\sum_{h_1}\sum_{h_2\neq h_1}\left[F(h_1)F(h_2)w(\tau,t,h_1,h_2)\sum_{n_1=0}^{N}\sum_{n_2=0}^{N}\left[x(t,n_1,h_1)x^*(t-\tau,n_2,h_2)e^{i\omega_{n_2h_2}\tau}\right]\right]\right\}=$$

$$=\sum_{t=\tau}^{T}\left\{\sum_{h,\,h_2=h_1}\left[F^2(h)w(\tau,t,h,h)\sum_{n,\,n_1=n_2}^{N}x^2(t,n,h)\right]\right\}+$$

$$+\sum_{t=\tau}^{T}\left\{\sum_{h,\,h_2=h_1}\left[F^2(h)w(\tau,t,h,h)\sum_{n_1=0}^{N}\sum_{n_2\neq n_1}^{N}\left[x(t,n_1,h_1)x^*(t-\tau,n_2,h_2)e^{i\omega_{n_2h_2}\tau}\right]\right]\right\}+$$

$$+\sum_{t=\tau}^{T}\left\{\sum_{h,\,h_2=h_1}\left[F^2(h)w(\tau,t,h,h)\sum_{n_1=0}^{N}\sum_{n_2\neq n_1}^{N}\left[x(t,n_1,h_1)x^*(t-\tau,n_2,h_2)e^{i\omega_{n_2h_2}\tau}\right]\right]\right\}+$$

$$+\sum_{t=\tau}^{T}\left\{\sum_{h_1}\sum_{h_2\neq h_1}\left[F(h_1)F(h_2)w(\tau,t,h_1,h_2)\sum_{n_1=0}^{N}\sum_{n_2=0}^{N}\left[x(t,n,h_1)x^*(t-\tau,n,h_2)e^{i\omega_{nh_2}\tau}\right]\right]\right\}+$$

$$\sum_{t=\tau}^{T}\left\{\sum_{h_1}\sum_{h_2\neq h_1}\left[F(h_1)F(h_2)w(\tau,t,h_1,h_2)\sum_{n_1=0}^{N}\sum_{n_2\neq n_1}^{N}\left[x(t,n_1,h_1)x^*(t-\tau,n_2,h_2)e^{i\omega_{n_2h_2}\tau}\right]\right]\right\}.$$

REFERENCES

Alsatkin S.S., Medvedev A.V., Kushnarev D.S. Analyzing the characteristics of phase shift keyed signals applied to the measurement of an electron concentration profile using the radiophysical model of the ionosphere. *Geomagnetism and Aeronomy.* 2009. vol. 49, no. 7 (Special Iss. 1). pp. 1022–1027. DOI: 10.1134/S0016793209070305.

Berngardt O.I., Kushnarev D.S. Effective subtraction technique at the Irkutsk Incoherent Scatter Radar: Theory and experiment. *J. Atmosph. Solar-Terr. Phys.* 2013, vol. 105–106, pp. 293–298. DOI: 10.1016/j.jastp.2013.03.023.

Berngardt O.I., Potekhin A.P. Radar equations in the radio wave backscattering problem. *Radiophysics and quantum electronics.* 2000. vol. 43, iss. 6, pp. 484–492. DOI: 10.1007/BF02677176.

Dougherty J.P., Farley D.T. A theory of incoherent scatter of radio waves by a plasma. *J. Geophys. Res.* 1963, vol. 66, no. 19, pp. 5473–5486.

Evans J.V. Theory and practice of Ionosphere study by Thomson scatter radar. *Proc. IEEE.* 1969, vol. 57, no. 4,

pp. 496–530. DOI: 10.1109/PROC.1969.7005.

Farley D.T. Incoherent scatter correlation function measurements. *Radio Sci.* 1969, vol. 4, no. 10, pp. 935–953. DOI: 10.1029/RS004i010p00935.

Holt J.M., Rhoda D.A., Tetenbaum D., van Eyken A.P. Optimal analysis of incoherent scatter radar data. *Radio Sci.* 1992, vol. 27, no. 3, pp. 435–447. DOI: 10.1029/91RS02922.

Hysell D.L., Rodrigues F.S., Chau J.L., Huba J.D. Full profile incoherent scatter analysis at Jicamarca. *Annales Geophysicae.* 2008. vol. 26, iss.1, pp. 59–75. DOI: 10.5194/angeo-26-59-2008.

Kudeki E., Milla M.A. Incoherent scatter radar — spectral signal model and ionospheric applications. *Doppler Radar Observations — Weather Radar, Wind Profiler, Ionospheric Radar, and Other Advanced Applications.* InTech, 2012, Chap. 16, pp. 377–406. DOI: 10.5772/2036.

Lentinen M.S. Statistical theory of incoherent scatter radar measurements: Ph.D. Thesis. University of Helsinki, 1986, pp. 25–28.

Medvedev A.V. *Razvitie metodov i apparatnykh sredstv radiofizicheskikh issledovanii verkhnei atmosfery Zemli na*

Irkutskom radare nekogerentnogo rasseyaniya [Development of methods and hardware of radiophysical investigations of Earth's upper atmosphere at the Irkutsk Incoherent Scatter Radar]. Dr. Phys. and Math. Sci. Diss. Irkutsk, 2014. 225 p. (In Russian).

Potekhin A.P., Medvedev A.V., Zavorin A.V., Kushnarev D.S., Lebedev V.P., Lepetaev V.V., Shpynev B.G. Recording and control digital systems of the Irkutsk Incoherent Scatter Radar. Geomagnetism and Aeronomy. 2009, vol. 49, iss. 7, pp. 1011–1021. DOI: 10.1134/S0016793209070299.

Rogozhkin E.V. Measuring parameters of ionospheric plasma from correlation function of incoherent scatter sign al. *Ionosfernye issledovaniya* [Ionospheric Res.] 1979, vol. 27, pp. 46–59.

Ratovsky K.G., Dmitriev A.V., Suvorova A.V., Shcherbakov A.A., Alsatkin S.S., Oinats A.V. Comparative study of COSMIC/FORMOSAT-3, Irkutsk incoherent scatter radar, Irkutsk Digisonde and IRI model electron density vertical profiles. *Adv. Space Res.* 2017, vol. 60, pp. 452–460. DOI: 10.1016/j.asr.2016.12.026.

Sheffield J. *Plasma Scattering of Electromagnetic Radiation*. 1st Edition. Academic Press, 1975. 318 p. DOI: 10.1016/C2013-0-07592-5

Shpynev B.G. Incoherent scatter Faraday rotation measurements on a radar with single linear polarization. *Radio Sci.* 2004, vol. 39, no. 3, pp. 1–8. DOI: 10.1029/2001RS002523.

Tarantola A. Inverse Problem Theory. 1st Edition. New York, Elseiver Science, 1987, 644 p.

Vasilyev R.V., Artamonov M.F., Beletsky A.B., Zherebtsov G.A., Medvedeva I.V., Mikhalev A.V., Syrenova T.E. Registering upper atmosphere parameters in East Siberia with Fabry—Perot Interferometer KEO Scientific "Arinae". Solar-Terr.Phys. 2017, vol. 3, no. 3, pp. 61–75. DOI: 10.12737/stp-33201707.

Zherebtsov G.A., Zavorin A.V., Medvedev A.V., Nosov V.E., Potekhin A.P., Shpynev B.G. Irkutsk Incoherent Scatter Radar. *Radiotekhnika i elektronika* [J. of Communications Technology and Electronics]. 2002, vol. 47, 11, pp. 1339–1345. (In Russian).

URL: http://hpc.icc.ru (accessed May 22, 2018).
URL: http://ckp-rf.ru/usu/77733 (accessed May 22, 2018).